Temperature-induced spin density wave in a magnetically doped topological insulator Bi_2Se_3

Martha Lasia and Luis Brey
Instituto de Ciencia de Materiales de Madrid, (CSIC), Cantoblanco, 28049 Madrid, Spain
(Received 9 March 2012; revised manuscript received 8 June 2012; published 19 July 2012)

We study the magnetic properties of Bi_2Se_3 doped with isoelectronic magnetic impurities. We obtain that at zero temperature the impurities order ferromagnetically, but when raising the temperature the system undergoes a first-order phase transition to a spin density wave phase before the system reaches the paramagnetic phase. The origin of this phase is the nontrivial dependence of the spin susceptibility on the momentum. We analyze the coupling of the nonuniform magnetic phase with the Dirac electronic system that occurs at the surfaces of the topological insulator.

DOI: 10.1103/PhysRevB.86.045317 PACS number(s): 72.25.Dc, 73.20.−r, 73.50.−h

I. INTRODUCTION

Topological insulators (TIs) are a newly discovered type of systems which are insulating in the bulk and characterized by the existence of a robust helical gapless Dirac two-dimensional electron system at their surface.[1–3]

TIs are typically band insulators for which strong spin-orbit coupling produces an inversion of the bulk band gap. Therefore, in TIs the energy gap is related to the spin-orbit coupling and that limits its magnitude. The most studied and more promising topological insulator is Bi_2Se_3, which is a three-dimensional TI with a relatively large bulk energy gap ($\sim$0.3 eV) and with the Dirac point of the surface states located outside the bulk bands.[4,5] Angle resolved spectroscopy[4,6] and scanning tunneling microscopy[7] experiments have shown the Dirac nature of the surface states of Bi_2Se_3.

The spin and wave vector of the surface states of a TI are strongly coupled, and the occurrence of a half-quantized Hall effect when an energy gap opens at the surface has been predicted.[8,9] Due to the protected character of the Dirac states, a gap at the surface should be opened with a perturbation that breaks the time reversal symmetry. This can be done by doping the system with magnetic impurities. At the surface of the TI, because of the large spin-orbit coupling, the interaction between the Dirac-like surface states and the impurities induces a large single ion magnetic anisotropy and polarizes the spin of the impurities perpendicularly to the surface. This spin-orbit coupling translates in the opening of an energy gap at the Dirac point of the surface states.[10–19]

From the experimental side, angle resolved photoemission spectroscopy (ARPES) studies on the surface of Fe-doped Bi_2Se_3 single crystals have confirmed the opening of an energy gap at the Dirac point[20] and the creation of odd multiples of Dirac fermions.[21] Also, recently, experiments in thin films of Cr-doped $Bi_xSb_{2-x}Te_3$ have shown a large anomalous Hall conductance in a magnetically doped topological insulator.[22]

However, recent experiments[23] found that the spins of Fe ions deposited on Bi_2Se_3 orient in-plane. Also ARPES experiments[24,25] found Dirac crossing even in the presence of magnetic impurities in contradiction with earlier experiments and existing theory. On the other hand, recently the suppression of the Dirac point spectral weight, both in magnetically doped and undoped TI, suggesting that the observed gap at the Dirac point cannot be taken as the sole evidence of a magnetic gap has been reported.[26] In addition, density functional theory based calculations[27] find that Co adatoms lying in the Bi_2Se_3 surface exhibit an energetically stable magnetic moment perpendicular to the surface, whereas for Co atoms located on the interlayer van der Waals spacing the momentum is in the plane parallel to the surface. All these results indicate the complexity of the interpretation of the ARPES experiments and the possible importance of other effects not included in the Dirac Hamiltonian, as crystalline anisotropy or surface reconstruction might play an important role on the orientation of the magnetic impurities. In this work we use an effective Hamiltonian for describing Bi_2Se_3, which although it does not include microscopic details of the material, describes appropriately the basic properties of the Bi_2Se_3 related to its band structure topology.

In this work we study the phase diagram of magnetically doped Bi_2Se_3. Bi_2Se_3 is a layered material formed by five atom layers arranged along the z direction. We find that at low temperatures the magnetic impurities order ferromagnetically along the z direction. By raising the temperature, the TI undergoes two transitions. A first-order transition from the ferromagnetic to the spin density wave phase and at higher temperatures a second-order transition from the spin density wave phase to the paramagnetic phase. The spin density wave phase has both the polarization and the wave vector parallel to the z direction. We have also studied the effect of the surface states by calculating the magnetization as a function of temperature of a slab of Bi_2Se_3 topological insulator. Here we find that the surface magnetization survives to higher temperatures than the bulk spin density wave phase.

The paper is organized as follows. In Sec. II we define the Hamiltonian we use for describing the electrical properties of Bi_2Se_3. In Sec. III we calculate the wave vector dependent paramagnetic spin susceptibility of Bi_2Se_3 and discuss the interaction between magnetic impurities through the paramagnetic susceptibility. In Sec. IV we formulate a Landau theory for describing the magnetic order of magnetically doped Bi_2Se_3, and discover the existence of a ferromagnetic to spin density wave phase transition at finite temperature. In Sec. V we study the polarization profiles of a magnetically doped Bi_2Se_3 slab and analyze the effect that the Dirac-like surface states have on the magnetic phases. We finish in Sec. VI with some conclusions and remarks.

II. HAMILTONIAN

The low energy and long wavelength electronic properties of Bi_2Se_3 topological insulators are described by the four bands $\mathbf{k}\cdot\mathbf{p}$ Hamiltonian,[5]

$$H = E(\mathbf{k}) + \mathcal{M}(\mathbf{k})\tau_z \otimes I + A_1 k_z \tau_x \otimes \sigma_z + A_2(k_x\tau_x + k_y\tau_y)\otimes\sigma_x, \quad (1)$$

where σ_v and τ_v are Pauli matrices, I is the unity matrix, $\mathcal{M}(\mathbf{k}) = M_0 - B_2(k_x^2+k_y^2) - B_1 k_z^2$, $k_\pm = k_x \pm i k_y$, and $E(\mathbf{k}) = C + D_1 k_z^2 + D_2(k_x^2+k_y^2)$. The Hamiltonian is written in the basis $|1\rangle = |p1_z^+,\uparrow\rangle$, $|2\rangle = -i|p2_z^-,\uparrow\rangle$, $|3\rangle = |p1_z^+,\downarrow\rangle$, $|4\rangle = i|p2_z^-,\downarrow\rangle$, which are the hybridized states of the Se p orbital and the Bi p orbital with even (+) and odd (−) parities and spin up (↑) and down (↓). The Hamiltonian parameters for Bi_2Se_3 are[28] $M_0 = 0.28$ eV, $A_1 = 0.22$ eV nm, $A_2 = 0.41$ eV nm, $B_1 = 0.10$ eV nm^2, $B_2 = 0.566$ eV nm^2, $C = -0.0068$ eV, $D_1 = 0.013$ eV nm^2, and $D_2 = 0.196$ eV nm^2. In this basis the spin operators get the form[29] $S_z = I\otimes\sigma_z$, $S_x = \tau_z\otimes\sigma_x$, and $S_y = \tau_z\otimes\sigma_y$.

III. BULK SPIN SUSCEPTIBILITY

The paramagnetic susceptibility obtained from the Hamiltonian Eq. (1) has the form

$$\chi_{\mu\mu}(\mathbf{q}) = \frac{2}{\Omega}\sum_{\substack{n' \text{ occ.}\\ n \text{ empty}}}\sum_{\mathbf{k}}\frac{|\langle n',\mathbf{k}+\mathbf{q}|S_\mu|n,\mathbf{k}\rangle|^2}{\varepsilon_{n',\mathbf{k}+\mathbf{q}} - \varepsilon_{n,\mathbf{k}}}. \quad (2)$$

Here $|n,\mathbf{k}\rangle$ and $\varepsilon_{n,\mathbf{k}}$ are the eigenfunctions and eigenvalues of Hamiltonian Eq. (1) and Ω is the sample volume. In the case of an insulator, this spin susceptibility is caused by the coupling of the valence and conduction band induced by the spin operator.[30] The susceptibility is a smooth function of the wave vector and because the system is an insulator there are no anomalies associated with Fermi surfaces. The symmetry of the original Hamiltonian dictates that the nondiagonal elements of the susceptibility tensor are zero and $\chi_{xx} = \chi_{yy} \neq \chi_{zz}$.

In Fig. 1 we plot the χ_{xx} and χ_{zz} as a function of q_z and q_x. The direct coupling $A_2 k_\pm$, between atomic orbitals with opposite parities and opposite z component of the spin, makes that for $k_\pm \neq 0$, occupied and empty states are coupled through S_z. Whereas those states are only connected through S_x when $k_z \neq 0$. This makes $\chi_{zz}(\mathbf{q}) > \chi_{xx}(\mathbf{q})$.

The more important contribution to $\chi_{zz}(q_z)$ comes from regions in the reciprocal space where the matrix elements $\langle n',\mathbf{k}+q_z|S_z|n,\mathbf{k}\rangle|$, with n occupied and n' empty, reaches the maximum value. This happens when $\mathcal{M}(\mathbf{k}) = 0$ or $\mathcal{M}(\mathbf{k}+q_z) = 0$. For a given k_z these conditions define two circular crowns of radius $\sqrt{\frac{M_0 - B_1 k_z^2}{B_2}}$ and $\sqrt{\frac{M_0 - B_1(k_z+q_z)^2}{B_2}}$ and thickness $A_2/(2B_2)$. Therefore, the area of the reciprocal space that contributes appreciably to $\chi_{zz}(q_z)$ increases with q_z. For larger values of q_z one of the circular crowns collapses to zero and the contributions to the integral decrease. This behavior explains qualitatively the maximum that χ_{zz} presents at a wave vector $G \sim \sqrt{M_0/B_1}$.

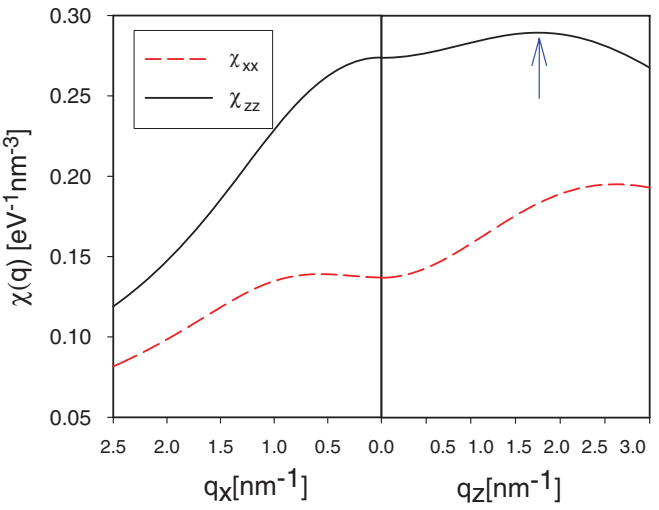

FIG. 1. (Color online) Spin susceptibility as a function of the wave vector along the z and the x directions. The arrow indicates the position of the maximum.

The existence of a maximum in $\chi_{zz}(\mathbf{q_z})$ at finite q_z is robust against small changes in the parameters of the four bands Hamiltonian. In Fig. 2 we plot $\chi_{zz}(\mathbf{q_z})$ for different values of the TI gap. The position of the maximum decreases continuously towards $q = 0$ when M_0 decreases and only disappears for small values of M_0. In the normal insulator phase $M_0 < 0$, the maximum always occurs at $q = 0$.

A. Coupling between diluted magnetic impurities

Consider now a TI doped with magnetic impurities of spin S. We assume that the number of electrons in the system does not change in the presence of the magnetic impurities. That can be achieved by doping with isoelectronic magnetic dopants or

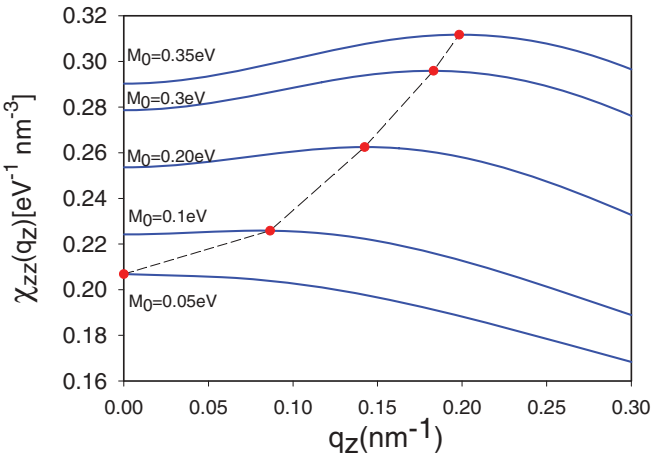

FIG. 2. (Color online) Spin magnetic susceptibility χ_{zz} for different values of M_0 as a function of the momentum in the z direction. All other parameters of the band structure correspond to those of Bi_2Se_3. As the value of the mass M_0 decreases the position of the maximum of the susceptibility moves towards small values of q_z. At small values of M_0 the maximum occurs at $q_z = 0$. In the normal insulator phase $M_0 < 0$, the maximum of χ_{zz} occurs at $q_z = 0$ for all values of the mass parameter. The dots indicate the position of the maximum.

by adding compensating nonmagnetic dopants.[31] In this work we consider the dilute limit, that is, concentration of impurities smaller than 5%, for which the direct interaction between the spin of the magnetic impurities can be neglected.

However, the electrons spins have a strong exchange coupling $\frac{S}{2}\tilde{J}(|\mathbf{r}|)$ with the magnetic impurities spins, which, in turn, are equally affected by the exchange field of the electrons. In this form the magnetic impurities in the system interact mediated by electronic states. We treat this interaction in second-order perturbation theory[32,33] that has proved to be a reliable approximation in diluted magnetic semiconductors.[33,34] In this approach the effective exchange parameter between two magnetic impurities separated by a vector $\mathbf{R}$ and spins pointing in the ν direction is

$$J_\nu(\mathbf{R}) = -\frac{S^2}{4} J_{\text{eff}}^2 \Omega \sum_{\mathbf{q}} \chi_{\nu\nu}(\mathbf{q}) e^{i\mathbf{qR}}, \tag{3}$$

where $J_{\text{eff}} = \int \tilde{J}(|\mathbf{r}|) d\mathbf{r}$ is the effective exchange coupling between the magnetic impurity and the electron spin.

Because $\chi_{zz} > \chi_{xx}$ in all range of wave vectors, the system has an easy axis of magnetization along the z direction and therefore isoelectronic magnetic impurities in Bi_2Se_3 will tend to polarize in the z direction. The maximum that the spin susceptibility presents at finite wave vector in the z direction will determine the existence of nonuniform polarization in magnetically doped TI. We treat the magnetically ordered state in the virtual crystal approximation,[32,33,35,36] and we consider that the system is invariant in the (x,y) plane, and the polarization only depends on the z direction. In the next section we obtain the magnetic polarization as a function of temperature and z coordinate by using a Landau free-energy functional.

IV. LANDAU FREE-ENERGY FUNCTIONAL

We assume that the system is invariant in the (x,y) plane, and allow the polarization to oscillate with period $2\pi/G$ along the z direction. In consequence we define the normalized magnetic polarization $-1 \leqslant m(z,T) \leqslant 1$ as

$$m(z,T) = m_0(T) + m_G(T)\cos(Gz), \tag{4}$$

where m_0 and m_G are the order parameters of the uniform ferromagnetic (FM) phase and the spin density wave phase (SDW), respectively.

The internal energy per unit volume corresponding to this magnetization is

$$E = -\frac{J}{2} m_0^2 \chi_{zz}(0) - \frac{J}{4} m_G^2 \chi_{zz}(G), \tag{5}$$

where $J = \frac{S^2}{4} J_{\text{eff}}^2 c$, c being the density of magnetic impurities. In our case, the value of $\chi_{zz}(G)$ is less than 10% larger than $\chi_{zz}(0)$ and the zero temperature ground state is a uniform FM phase, $m(z,T=0)=1$. However the maximum of the spin susceptibility at G will modify the spin density at larger temperatures.

Knowing that for small values of the polarization the entropy of a classical spin at a given T is (see the Appendix)

$$-TS = -k_B T \ln(2) + \tfrac{3}{2} k_B T m^2 + \tfrac{9}{20} k_B T m^4. \tag{6}$$

We get that in the mean-field approximation and for small values of magnetic polarization the Landau free energy per unit volume takes the form

$$\mathcal{F} = -\frac{J}{2} m_0^2 \chi_{zz}(0) - \frac{J}{4} m_G^2 \chi_{zz}(G) - \frac{1}{\beta}\frac{1}{L}\int dz \left[\ln 2 - \frac{3}{2} m^2(z,T) - \frac{9}{20} m^4(z,T) \cdots \right], \tag{7}$$

where $\beta = 1/k_B T$ and L is the sample dimension in the z direction. Using expression (4), and in the limit $L \to \infty$, we get

$$\mathcal{F} = \tfrac{3}{2} m_0^2 k_B (T - T_0) + \tfrac{3}{4} m_G^2 k_B (T - T_G) + k_B T \tfrac{27}{20} m_0^2 m_G^2 + k_B T \tfrac{9}{20} m_0^4 + k_B T \tfrac{27}{160} m_G^4, \tag{8}$$

where T_0 and T_G are the critical temperatures of the pure FM and SDW phases, respectively,

$$k_B T_0 = \frac{J}{3}\chi_{zz}(0) \quad \text{and} \quad k_B T_G = \frac{J}{3}\chi_{zz}(G). \tag{9}$$

The phase diagram of a system described by a free energy as that of Eq. (8) depends on the relative magnitudes of the fourth-order potentials.[37] In our case the product of the prefactors of m_0^4 and m_G^4 is smaller than the square of the $m_0^2 m_G^2$ prefactor and there is no phase coexistence in the phase diagram. By increasing the temperature, there is a first-order transition from the FM phase to the SDW phase at

$$T^* = \frac{\sqrt{3}T_0 - \sqrt{2}T_G}{\sqrt{3} - \sqrt{2}}. \tag{10}$$

This is the main result of this work: By heating, a magnetically doped TI undergoes two phase transitions, a FM to SDW first-order transition at T^* and a SDW to paramagnetic second-order transition at T_G. Although at $T = 0$ the FM phase has lower energy than the SDW phase, the FM to SDW transition at finite T occurs because the entropy of the SDW increases faster with T than the entropy of the FM phase.

In the next section we analyze how the surface states existing in topological insulators couple to the bulk magnetic polarization.

V. SPIN POLARIZATION OF MAGNETICALLY DOPED TI SLABS

At the surface of a TI there exists a two-dimensional Dirac electron gas. Because of the chirality of the electron gas, an exchange field perpendicular to the surface opens a gap in the spectra. Then, in order to minimize the energy, a magnetic impurity will polarize perpendicularly to the surface.[10–12,18] In the diluted limit, surface states mediate a Ruderman-Kittel-Kasuya-Yosid (RKKY) interaction among the impurities which is always ferromagnetic, whenever the chemical potential resides near the Dirac point.[10,12,18,38] Therefore magnetic impurities at the surface of a TI will order ferromagnetically perpendicular to the surface.

We are going to study numerically the spin polarization as a function of temperature and position of a magnetically doped TI slab. The objective here is first to confirm the results obtained with the Landau functional where we consider a

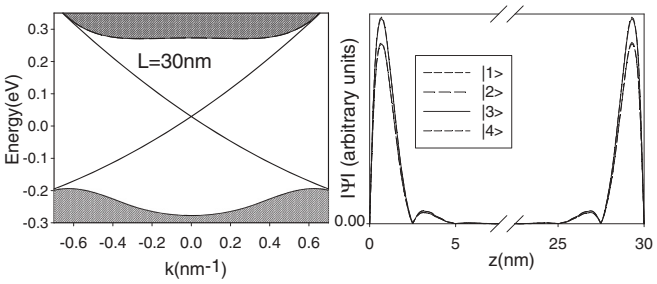

FIG. 3. In the left panel we plot the band structure of a topological insulator film 30 nm thick. For this thickness there is no coupling between localized states on opposite surfaces and surface states are degenerated. Dashed areas denote the bulk band structure. In the right panel we plot the absolute value of the four components of the wave function of a surface state with momentum close to zero.

unique Fourier component of $\chi_{zz}(q_z)$ and second to analyze the coupling between the surface and the bulk magnetization.

We analyze a TI slab of thickness L perpendicular to the z direction. We expect the electron affinity of Bi_2Se_3 to be much larger than its band gap. Therefore, at the surface of the TI we will neglect the penetration of the electron wave function into the vacuum. The eigenvalues $\varepsilon_{n,\mathbf{k}}$ and wave functions $\Psi_{n,\mathbf{k}}(z)$ are obtained by solving Eq. (1) with $k_z = -i\partial_z$ and forcing the wave function to vanish at $z = 0$ and $z = L$. This is satisfied expanding $\Psi_{n,\mathbf{k}}(z)$ in harmonics,

$$\Psi_{n,\mathbf{k}}(z) = \frac{e^{i\mathbf{kr}}}{\sqrt{A}}\sqrt{\frac{2}{L}}\sum_{l=1}^{N_{\max}}\sum_{j=1,4} a^l_{n,j}(\mathbf{k})\sin\left(\frac{l}{L}\pi z\right), \quad (11)$$

here A is the sample area and we choose $N_{\max}$ large enough so that the results do not depend on it.

For $L > 10$ nm the surfaces of the slab are decoupled and the band structure is independent of L. In the bulk energy gap region, some surface states appear which are the benchmark of the TI. In Fig. 3 we plot the band dispersion and the shape of the wave function of these states. The results we obtain agree completely with previous results.[3,29]

In the slab geometry the momentum in the z direction is not a good quantum number and the paramagnetic susceptibility depends on two position indices z and z'. Therefore, in the virtual crystal approximation and in second-order perturbation theory, the internal energy of the magnetically doped TI slab is

$$E = \frac{J}{2L}\int_0^L\int_0^L dz dz' \tilde{\chi}(z,z')m(z)m(z'), \text{ with} \quad (12)$$

$$\tilde{\chi}(z,z') = \frac{1}{A}\sum_{n,n',\mathbf{k}}\frac{n_F(\varepsilon_{n,\mathbf{k}}) - n_F(\varepsilon_{n',\mathbf{k}})}{\varepsilon_{n',\mathbf{k}} - \varepsilon_{n,\mathbf{k}}} \times \Psi^*_{n,\mathbf{k}}(z)S_z\Psi_{n',\mathbf{k}}(z) \times \Psi^*_{n',\mathbf{k}}(z')S_z\Psi_{n,\mathbf{k}}(z'), \quad (13)$$

where $n_F(\varepsilon)$ is the Fermi distribution function. $\tilde{\chi}(z,z')$ indicates the coupling between uniform polarized (x,y) planes, located at positions z and z'. The interaction between magnetic impurities is mediated by electrons in the system, and because the bulk system is an insulator, the interaction is very short ranged in the z direction, see Fig. 4.

We compute the temperature dependence of the magnetization profile in the mean-field approximation. At a given position z, the magnetization $m(z,T)$ feels a (in energy units)

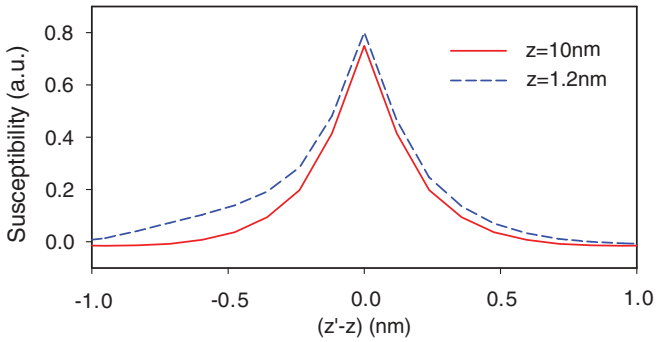

FIG. 4. (Color online) $\tilde{\chi}_{zz}(z,z')$ evaluated at the maximum of the surface wave function, $z = 1.2$ nm, and at the center of a 20 nm thick slab, as a function of z'. The first case corresponds to a region near the surface, where the two-dimensional Dirac electron system contributes to the response functions. In the latter case the response function is not affected by the surface and it is the bulk response function. In both cases the functions are very peaked at $z = z'$. The negative values of the coupling in the bulk response function is a consequence of the maximum that the response function present at $q_z = G$ in the reciprocal space. Near the surfaces, and because of their metallic character, the magnetic coupling is stronger. This is reflected in the asymmetry of the dashed line, the interaction between planes is larger the closer the planes are to the surface.

magnetic field,

$$B(z) = J\int_0^L dz'\tilde{\chi}(z,z')m(z'), \quad (14)$$

and the magnetization of an isolated impurity in the presence of the molecular field is

$$m(z,T) = \coth\left[\frac{B(z)}{k_BT}\right] - \frac{k_BT}{B}. \quad (15)$$

Solving self-consistently Eqs. (14) and (15), we obtain the magnetization profiles as a function of T.

Because the metallic surface states intermediate a RKKY coupling[10,38] at the surface, the response function $\tilde{\chi}(z,z')$ is larger near the surface than in the bulk, see Fig. 4. Therefore, as function of T, the absolute value of the magnetization decreases faster in the bulk region than in the surface.[39] However, it is important to note that the surface and the bulk are part of a unique system and therefore there is only a *unique critical temperature* corresponding to the transition of the paramagnetic phase.

In Fig. 5 we show the magnetization as a function of temperature for TI slabs of thickness $L = 5$ nm, $L = 10$ nm, and $L = 30$ nm. We plot the average value of $m(z,T)$, and the value of the magnetization on top of the surface states. In Fig. 6 we plot the magnetization profiles for different temperatures and $L = 5$ nm, $L = 10$ nm, and $L = 30$ nm.

For $L = 10$ nm and $L = 30$ nm the surfaces are practically decoupled and the central part of the slab behaves as bulk. There is a strong jump in the magnetization at T^* that indicates the first-order FM to SDW transition. In the SDW phase the oscillating magnetization does not contribute to the total magnetization and the magnetization for $T > T^*$ is due to surface states. In Figs. 6(b) and 6(c) the abrupt transition from an uniform magnetization phase to a SDW phase is

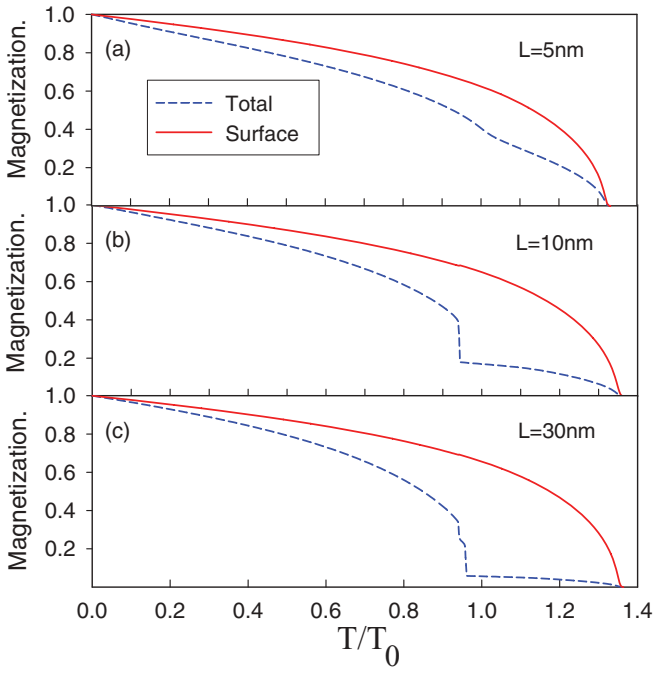

FIG. 5. (Color online) Magnetization as a function of temperature for TI slabs of thickness (a) $L = 5$ nm, (b) $L = 10$ nm, and (c) $L = 30$ nm. T_0 is the bulk FM critical temperature of the topological insulator. The small "step" in the middle of the first-order transition that occurs at $L = 30$ nm is a consequence of an interference effect between the surface magnetization and the bulk SDW phase.

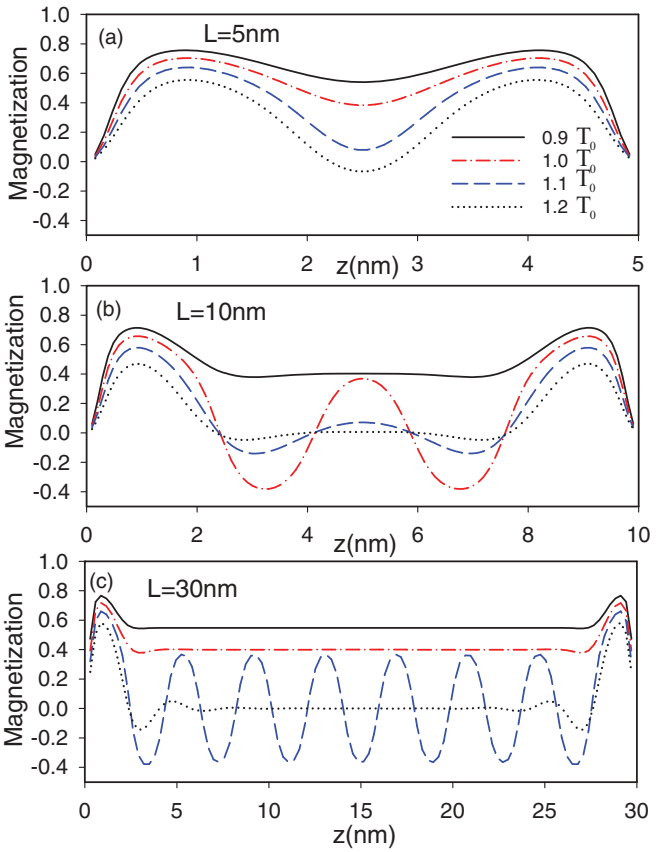

FIG. 6. (Color online) Magnetic polarizations as a function of the position across the topological insulator slab z for different layer thickness and temperatures.

apparent at the center of the slab. For smaller thickness of the slab [Fig. 6(a)] the surface states are coupled and there is no well-defined bulk region that reflects in the absence of FM to SDW transition.

The magnetization at the surface is practically not affected by the FM to SDW transition, and decays with T continuously to zero. The ferromagnetism at the surface is more robust than in the central part. For temperatures where m_0 and m_G are near zero, the surface of the system can be more than 30% polarized. These results indicate the possibility that the magnetization at the surfaces of TIs could be finite at temperatures larger than the bulk critical temperatures T_G and T^*.[39] Because of the metallic character of the TI surface states, there is a range of temperatures for which the Dirac-like electron system at the surface of the TI is gapped, although the bulk part of the system is practically unpolarized.

A similar SDW phase has been also obtained numerically by Rosenberg and Franz in a slab geometry of Bi_2Se_3.[39] However these authors interpret the oscillation of the polarization as spatial fluctuations of the bulk magnetization coupled with the surface magnetization. From our calculation we attribute the oscillations in the magnetization reported in Ref. 39 as a signature of the bulk SDW phase.

VI. FINAL REMARKS AND CONCLUSIONS

In this work we study the phase diagram of magnetically doped Bi_2Se_3. At low temperatures the magnetic impurities order ferromagnetically along the z direction. By raising the temperature, the TI undergoes two transitions. A first-order transition from the ferromagnetic to the spin density wave phase and at higher temperatures a second-order transition from the spin density wave phase to the paramagnetic phase. This result could explain recent experimental results[40] that suggest the existence, as function of the temperature, of two different magnetic phases in Fe doped Bi_2Se_3.

We have also studied the effect of the surface states by calculating the magnetization as a function of temperature of a slab of Bi_2Se_3 topological insulator. Here we find that the surface magnetization survives to higher temperatures than the bulk spin density wave phase. The existence of a range of temperatures for which the bulk magnetization practically vanishes, whereas a finite magnetization exits at the surface, could explain some experimental results that observe a gap at the surface of Bi_2Se_3 but not bulk magnetism.[20,21]

It is important to analyze the behavior of the phase diagram as a function of the gap parameter M_0. In Fig. 7 we show the phase diagram of a magnetically doped thick TI slab as a function of M_0. For $M_0 < 0$ the system is a normal insulator and there are no surface states. Also the spin-orbit coupling is small and the SDW phase does not exist. For $M_0 > 0$ the system is a TI and the gap increases with M_0. TI with larger gaps have more metallic surface states and the FM order at the surface is therefore more robust. Also the effective spin-orbit coupling is stronger and both T^* and T_G increase with M_0. The results of Fig. 7 show that the range of temperatures where the SDW phase exists increases with M_0.

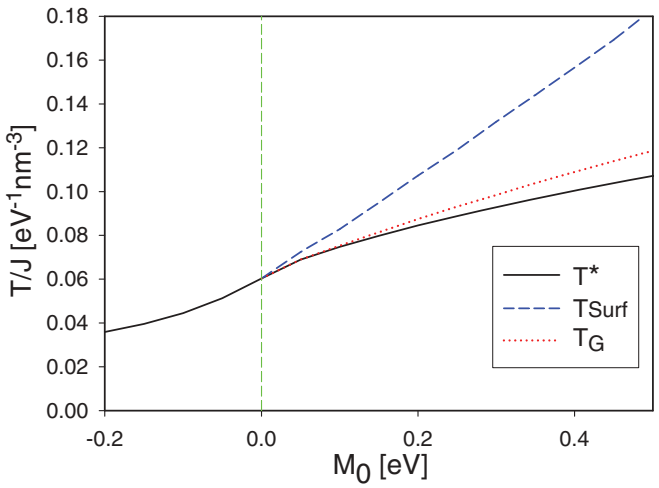

FIG. 7. (Color online) Phase diagram of a thick magnetic doped TI as a function of the mass parameter M_0.

Finally we make an estimation of the critical temperature. From the band structure parameters of Bi_2Se_3, choosing the density of the magnetic impurities to be 5×10^{20} cm^{-3}, the total angular momentum of a single magnetic ion to be $S = 3/2$, and the effective exchange coupling $J_{\rm eff} = 250$ meV nm^3 (Ref. 12) we obtain $T_G^{\rm bulk} \approx 18$ K. These values can change by factors of 2 by changing the magnetic ions or the density of impurities. It is well known that the mean-field approximations tend to overestimate the transition temperature due to the neglect of the fluctuations. In diluted magnetic semiconductors thermal fluctuations reduce the value of the Curie temperature in near 30%,[33] and we expect a similar reduction in topological insulators.

ACKNOWLEDGMENTS

We are very grateful to P. G. Silvestrov who called our attention to the correct definition of the spin matrices. We also acknowledge fruitful discussion with E. Chacón, H. A. Fertig, and A. H. MacDonald. Funding for this work was provided by MICINN-Spain via Grant FIS2009-08744.

APPENDIX: MEAN-FIELD EXPRESSION FOR THE ENTROPY

In this Appendix we obtain an expression for the entropy of a system of classical spins of magnetization m that are coupled with the topological insulator through a general term $E[m]$.

The free energy of a system of classical spins of magnitude unity in an external magnetic field h is

$$\mathcal{F} = -\frac{1}{\beta}\ln\left[2\frac{\sinh(\beta h)}{\beta h}\right], \tag{A1}$$

from where the magnetization can be calculated as

$$m \equiv \langle m\rangle = -\frac{\partial \mathcal{F}}{\partial h} = \frac{1}{\tanh(\beta h)} - \frac{1}{\beta h}. \tag{A2}$$

The entropy of the spin system is then

$$-TS = \mathcal{F} - mh = \frac{1}{\beta}\left\{-\ln\left[2\frac{\sinh(\beta h)}{\beta h}\right] - m\beta h\right\}. \tag{A3}$$

The total energy of the system is

$$\mathcal{F}^{\rm total} = E[m] - TS = E[m] - \frac{1}{\beta}\left\{\ln\left[2\frac{\sinh(\beta h)}{\beta h}\right] + m\beta h\right\}, \tag{A4}$$

where $E[m]$ is the change in the electronic energy of the system because of the polarization of the magnetic impurities.

To obtain h we minimize the total free energy with respect to h, $\partial\mathcal{F}^{\rm total}/\partial h = 0$. In the limit of small h,

$$\ln\left[2\frac{\sinh(\beta h)}{\beta h}\right] \simeq \ln(2) + \frac{(\beta h)^2}{6} - \frac{(\beta h)^4}{180} + \cdots. \tag{A5}$$

In this limit the minimization condition gives $\beta h = -3m - \frac{3}{5}m^3 + \cdots$, and the entropy gets the form

$$-TS = -k_B T\ln(2) + \frac{3}{2}k_{\rm B}Tm^2 + \frac{9}{20}k_{\rm B}Tm^4. \tag{A6}$$

[1] M. Z. Hasan and C. L. Kane, Rev. Mod. Phys. **82**, 3045 (2010).
[2] X.-L. Qi and S.-C. Zhang, Phys. Today **63**, 33 (2010).
[3] X.-L. Qi and S.-C. Zhang, Rev. Mod. Phys. **83**, 1057 (2011).
[4] L. Xia *et al.*, Nat. Phys. **5**, 398 (2009).
[5] H. Zhang *et al.*, Nat. Phys. **5**, 438 (2009).
[6] D. Hsieh *et al.*, Nature (London) **460**, 1101 (2009).
[7] T. Hanaguri, K. Igarashi, M. Kawamura, H. Takagi, and T. Sasagawa, Phys. Rev. B **82**, 081305 (2010).
[8] X.-L. Qi, T. L. Hughes, and S.-C. Zhang, Phys. Rev. B **78**, 195424 (2008).
[9] A. M. Essin, J. E. Moore, and D. Vanderbilt, Phys. Rev. Lett. **102**, 146805 (2009).
[10] Q. Liu, C.-X. Liu, C. Xu, X.-L. Qi, and S.-C. Zhang, Phys. Rev. Lett. **102**, 156603 (2009).
[11] R. R. Biswas and A. V. Balatsky, Phys. Rev. B **81**, 233405 (2010).
[12] R. Yu, W. Zhang, H.-J. Zhang, S.-C. Zhang, X. Dai, and Z. Fang, Science **329**, 61 (2010).
[13] J.-H. Jiang and S. Wu, Phys. Rev. B **83**, 205124 (2011).
[14] T. Yokoyama, Phys. Rev. B **84**, 113407 (2011).
[15] J.-J. Zhu, D.-X. Yao, S.-C. Zhang, and K. Chang, Phys. Rev. Lett. **106**, 097201 (2011).
[16] D. A. Abanin and D. A. Pesin, Phys. Rev. Lett. **106**, 136802 (2011).
[17] V. N. Men'shov, V. Tugushev, and E. Chulkov, JETP Lett. **94**, 629 (2011).
[18] A. Nunez and J. Fernández-Rossier, Solid State Commun. **152**, 403 (2012).
[19] T. Habe and Y. Asano, Phys. Rev. B **85**, 195325 (2012).
[20] Y. L. Chen *et al.*, Science **329**, 659 (2010).
[21] L. A. Wray *et al.*, Nat. Phys. **7**, 32 (2010).

[22]C.-Z. Chang, J.-S. Zhang, M.-H. Liu, Z.-C. Zhang, X. Feng, K. Li, L.-L. Wang, X. Chen, X. Dai, Z. Fang *et al*., arXiv:1108.4754.
[23]J. Honolka, A. A. Khajetoorians, V. Sessi, T. O. Wehling, S. Stepanow, J.-L. Mi, B. B. Iversen, T. Schlenk, J. Wiebe, N. Brookes *et al*., Phys. Rev. Lett. **108**, 256811 (2012).
[24]M. R. Scholz, J. Sánchez-Barriga, D. Marchenko, A. Varykhalov, A. Volykhov, L. V. Yashina, and O. Rader, Phys. Rev. Lett. **108**, 256810 (2012).
[25]T. Valla, Z.-H. Pan, D. Gardner, Y. S. Lee, and S. Chu, Phys. Rev. Lett. **108**, 117601 (2012).
[26]S.-Y. Xu, L. A. Wray, N. Alidoust, Y. Xia, M. Neupane, C. Liu, H.-W. Ji, S. Jia, R. J. Cava, and M. Z. Hasan, arXiv:1206.0278.
[27]T. M. Schmidt, R. H. Miwa, and A. Fazzio, Phys. Rev. B **84**, 245418 (2011).
[28]C.-X. Liu, X.-L. Qi, H. J. Zhang, X. Dai, Z. Fang, and S.-C. Zhang, Phys. Rev. B **82**, 045122 (2010).
[29]P. G. Silvestrov, P. W. Brouwer, and E. G. Mishchenlo, arXiv:1111.3650.
[30]J. Vleck, *The Theory of Electronic and Magnetic Susceptibilities* (Oxford University Press, London, 1932).
[31]Y. S. Hor, A. Richardella, P. Roushan, Y. Xia, J. G. Checkelsky, A. Yazdani, M. Z. Hasan, N. P. Ong, and R. J. Cava, Phys. Rev. B **79**, 195208 (2009).
[32]T. Dietl, H. Ohno, F. Matsukura, J. Cibert, and D. Ferrand, Science **287**, 1019 (2000).
[33]L. Brey and G. Gómez-Santos, Phys. Rev. B **68**, 115206 (2003).
[34]M. J. Calderón, G. Gómez-Santos, and L. Brey, Phys. Rev. B **66**, 075218 (2002).
[35]M. Abolfath, T. Jungwirth, J. Brum, and A. H. MacDonald, Phys. Rev. B **63**, 054418 (2001).
[36]J. Fernández-Rossier and L. J. Sham, Phys. Rev. B **64**, 235323 (2001).
[37]P. M. Chaikin and T. C. Lubensky, *Principles of Condensed Matter Physics* (Cambridge University Press, Cambridge, 1995).
[38]L. Brey, H. A. Fertig, and S. Das Sarma, Phys. Rev. Lett. **99**, 116802 (2007).
[39]G. Rosenberg and M. Franz, Phys. Rev. B **85**, 195119 (2012).
[40]Z. Salman, E. Pomjakushina, V. Pomjakushin, A. Kanigel, K. Chashka, K. Conder, E. Morenzoni, T. Prokscha, K. Sedlak, and A. Suter, arXiv:1203.4850.